Heat transfer and aroma modeling of fresh fruit and vegetable in cold chain: case study on tomatoes

Onrawee Laguerre, Alain Denis, Nadir Bouledjeraf, Steven Duret, Evelyne Derens-Bertheau, Jean Moureh, Christophe Aubert, Denis Flick

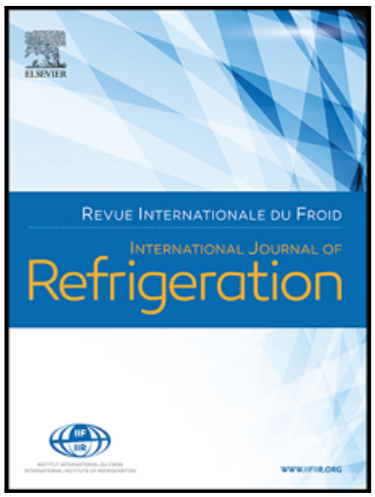

Heat transfer and aroma modeling of fresh fruit and vegetable in cold chain: case study on tomatoes

Onrawee Laguerre , Alain Denis , Nadir Bouledjeraf , Steven Duret , Evelyne Derens Bertheau , Jean Moureh , Christophe Aubert , Denis Flick

PII: S0140-7007(21)00403-5
DOI: https://doi.org/10.1016/j.ijrefrig.2021.10.009
Reference: JIJR 5324

To appear in: *International Journal of Refrigeration*

Received date: 22 March 2021
Revised date: 15 October 2021
Accepted date: 16 October 2021

Please cite this article as: Onrawee Laguerre , Alain Denis , Nadir Bouledjeraf , Steven Duret , Evelyne Derens Bertheau , Jean Moureh , Christophe Aubert , Denis Flick , Heat transfer and aroma modeling of fresh fruit and vegetable in cold chain: case study on tomatoes, *International Journal of Refrigeration* (2021), doi: https://doi.org/10.1016/j.ijrefrig.2021.10.009

Heat transfer and aroma modeling of fresh fruit and vegetable in cold chain: case study on tomatoes

Onrawee Laguerre[a,*], Alain Denis[a], Nadir Bouledjeraf[a,c], Steven Duret[a], Evelyne Derens Bertheau[a], Jean Moureh[a], Christophe Aubert[b], Denis Flick[c]

[a]Université Paris-Saclay, INRAE, FRISE, 92761 Antony, France

[b]Centre Technique Interprofessionnel des Fruits et Légumes (CTIFL), Route de Mollégès, F-13210 Saint-Rémy-de-Provence, France

[c]Université Paris-Saclay, INRAE, AgroParisTech, UMR SayFood, 91300 Massy, France

[*]Corresponding author:

1 rue Pierre-Gilles de Gennes, F-92761 Antony, France.

Tel: 00(33)1 40 96 62 96 Fax: 00(33)1 40 96 62 75 E-mail address: onrawee.laguerre@inrae.fr

Highlights

- Non uniform temperature in tomato crates arranged in a pallet layer was observed
- Simplified thermal and aroma models were developed and linked together
- Statistical analysis on these models showed acceptable Root Mean Square Error
- Aroma losses when temperature <12°C and recovers partially when return to ambient
- Product temperature and aroma evolutions in supply chain scenarios were predicted.

Abstract

Convective cooling/heating experiments were carried out using a device representing a half-layer of a pallet with four crates of tomatoes (var. Cauralina, *Solanum Lycopersicum*). Air and product temperatures were measured at different positions in the crates, which were exposed to several

different ambient conditions in order to study the influence of air velocity, warming/cooling regimes, hole opening area and filming. The experimental results show that the product and air temperatures vary with the distance from the air inlet position. Since airflow rate was varied and controlled using fans equipped with electrical power variation, a correlation between the air velocity and the convective heat transfer coefficient was established. A transient state heat transfer model was developed based on a zonal approach, which considers overall thermo-physical properties for each crate. An aroma model was developed based on three hypothetic first order kinetics. The model takes into account the observation reported in several studies that tomato aroma decreases when the product temperature is lower than 12 °C and the aroma is recovered, but only partially, when the product temperature is higher than 12 °C. Finally, the thermal model was linked with the aroma model to predict the product temperature and the aroma evolution in two examples of supply chain scenario from producer cold room to consumption point. These numerical results show that the tomato variety and the product time-temperature history in a supply chain exert a significant influence on the aroma evolution.

Keywords

modeling, heat transfer, aroma, pallet, supply chain

Nomenclature

A, B, C	Fraction of compound A (aroma), B and C, respectively
Bi	Biot number $= \frac{hR}{\lambda}$ [dimensionless]
C_p	Thermal capacity [J.Kg^{-1}.K^{-1}]
h	Convective heat transfer coefficient [W.m^{-2}.K^{-1}]
k_1, k_2 k_3	Kinetic parameters of aroma transformation [d^{-1}.K^{-1}]
m	Mass of one tomato [kg]

$\dot{m}$	Air mass flow rate [kg.s^{-1}]
n	Number of tomatoes in a crate
R	Radius [m]
S	Exchange area between product and air for one tomato [m^2]
T	Temperature (°C)
T*	Dimensionless temperature $\left[=\frac{T(t)-T_a}{T_0-T_a}\right]$
t	Time [s, min., h]
Va	Air velocity [m.s^{-1}]

Greek symbols

τ	Characteristic time (s)
ρ	Product density $[\mathrm{kg.m^3}]$
λ	Product thermal conductivity $[\mathrm{W.m^{-1}.K^{-1}}]$
τ	Characteristic time [s]

Subscripts

a	air
c	core
cri	critical
0	t = 0
p	product

1. Introduction

The product quality at the consumption point depends mainly on the product variety, maturity status at harvest, handling, packaging, postharvest refrigeration and storage temperature along the cold chain. Tomatoes are of particular interest in this study because their aroma and taste can be lost during cold storage. Inappropriate temperature in supply chain can explain the consumer complaints of less flavor in tomato nowadays in comparison with the one in the past. The recommended storage temperature of tomatoes is around 12 °C (Bai et al. 2011; Zhang, et al. 2008). When the temperature is too low, chilling injury and aroma loss may take place (Saltveit and Morris, 1990, Farneti et al., 2015) and the development of sugars and flavor is inhibited (de Leon-Sanchez et al., 2009). Gomez et al. (2009) found that tomato contains about 25 % less glucose when it is stored at 6 °C for 15 days in comparison with storage at 20 °C. Buttery et al. (1988) reported that there was a lack of volatile development when unripe tomatoes were stored under chilled conditions, and highlighted that the final ripening temperature was a determinant of odor intensity. Wang et al (2019) showed that the substantial volatile emission depends strongly on the maturity stage at harvest, it begins at pink stage and peaked at red stage. These authors reported that chilling strongly reduced volatile production even without visual chilling symptoms and they proposed heat treatment (52 ℃, 5 min) prior to chilling to maintain tomato fruit flavor quality. Several studies were carried out to analyze and characterize the volatile compounds of fruit and vegetable (Aubert et al, 2005; Raffo et al, 2018). However, the results of volatile compounds analysis may affected by the medium of evaluation (Tandon et al, 2000). In fact, these authors used 3 mediums (deionized water, ethanol/methanol/water mixture and a deodorized tomato homogenate) for the odor analysis. They noticed significant differences in aroma descriptors in different media. Jian et al (2019) have identified 36 volatile compounds in fresh tomatoes and reported different distribution of these compounds in tomato structure (pericarp, septa-columella, locular gel-seeds and stem end). Farneti et al. (2015) studied the effect of storage temperature variations on changes in aroma volatile compounds for several tomato varieties. The main volatile compounds responsible for tomato aroma

reported by these authors are Hexanal and trans-2-Hexanal. They found that when the product temperature decreases from room to refrigerator temperature, the abundance of most volatile compounds decreased significantly within three to five hours. When the product was restored to room temperature after several periods in cold storage, these volatile compounds increased again, but generally did not reach the original levels. Renard et al. (2013) reported that the concentration of volatile compounds had decreased by 66 % after 30 days at 4 °C, but some aroma was recovered after storage at a temperature of 20 °C for 24 h following cold storage for a period of up to 6 days.

Pham et al. (2019) carried out an experimental study and showed the relation between the air and product temperatures and the air velocity in a pallet loaded with cheese, which generated heat due to the fermentation reaction. These authors observed a lateral air outflow through the carton holes located on the side, which explained the poor ventilation and high temperature of the product located downstream from the flow in the pallet. Pham et al (2021) carried out a CFD modelling for a similar configuration (cheese pallet) taking into account forced convection and natural convection due to heat generated by product in a ventilated cold room. The model predicted precisely both the product temperatures and airflow patterns and can be used as a design tool to optimize the cooling system for different food product and packaging. Delele et al. (2013) also reported this observation, an air velocity decrease from the inlet towards the outlet of a crate and a temperature increase. They showed a 184 % increase in the cooling rate when the vent hole area increased from 1 % to 7 %. Airflow and product temperature inside a pallet are also greatly influenced by the airflow surrounding the pallet, which has been shown to be highly heterogeneous in cold chain contexts (Tapsoba et al. 2006; Chourasia and Goswani, 2007). Berry et al. (2017) showed the effect of carton vent hole design on the cooling efficiency and on the mechanical strength of the carton. Experimental and CFD (Computational Fluid Dynamic) studies demonstrated the influence of packaging design on its mechanical strength and on the refrigeration rate. Hoang et al (2015) used CFD approach to study the airflow and heat transfer in a cold room filled with four apple pallets. The comparison between numerical and experimental results (air/product temperatures and air velocity)

allowed the understanding of the airflow in the entire cold room in terms of magnitude and direction. However, CFD models require high numerical resource, as example, there are 4.2 x 10^5 cells for a refrigerated truck loaded by palettes and 3 days calculation with 450 MHz processor (Moureh and Flick, 2004). This makes the CFD fail to predict temperature in real-time while this is a key factor in providing operators with a decision support tool. Ambaw et al (2013) published a review article on studies using CFD approach to characterize and design post-harvest facilities. These studies investigate the flow, heat and mass transfer processes, which include complex aspects such as product stacking, gas diffusion and kinetics and droplet or particle dispersion.

According to our knowledge and for the majority of the available literature, the influence of storage temperature on the product quality was studied in laboratory on isolated product items and under constant temperature. These results cannot be applied directly to the cold chain along which, ambient temperature varies, in turn product temperature varies. This variation depends on the airflow conditions, on the position of product in the pallet and on other factors like packaging design. There is still a lack of knowledge, which link dynamically (via a transient state model) the product quality evolution, to the external airflow and temperature conditions like a pallet of fresh fruit or vegetable. Several transient states have to be considered in a supply chain, for example, when product is transferred from a supermarket cold room to display on shelves under room temperature or during loading/unloading in a refrigerated truck. A numerical tool allowing the prediction of the impact of supply chain condition on product quality can be useful for fruit and vegetable stakeholders. To develop this tool, several aspects are considered in this study.

In recent years, consumer claims about the decrease of fruit and vegetable taste, which is partly related to too low temperature in the postharvest chain until consumption. To answer to this ascertainment, this work aimed to evaluate the impacts of refrigeration and storage condition in postharvest supply chain of tomatoes on product quality. Concretely, the objectives of this study were (1) to study experimentally the influence on the product temperature changes at different positions in a pallet according to the ambient temperature variation, air velocity, hole area of the

cardboard crates and filming; (2) to develop a simplified transient heat transfer model to predict the product temperature changes in different positions in a pallet; and (3) to develop a product quality model to predict its evolution.

This study demonstrates that it is possible to combine relatively simple thermal and quality models to compare different scenarios of supply chain. As a first approach, our study case focuses on tomato aroma evolution. The thermal model was validated by comparing the predicted temperatures with experimental results, while the quality model was not yet validated. In fact, experimentation of tomato quality evolution under different supply chain conditions is in progress. These results will be used to validate the quality models and will be presented in our future article.

2. Materials and methods

2.1. Experimental device

The experimental device was installed in a temperature controlled test room of dimension 3m x 4m x 3m in which the temperature variation is < 0.2°C (calculated from 3 measure positions). The device representing a half-layer of tomatoes in a pallet was composed of 4 crates measuring 0.40 m x 0.3 m x 0.11 m (Fig. 1a). The studied tomato was Cauralina variety (*Solanum Lycopersicum*) with average diameter of 8.8 cm, average weight of 307 g/tomato and water content of 94 %. Twelve tomatoes were arranged in each crate (Fig.1b). Polystyrene plates (0.04 m thickness) were placed at the top, bottom and right sides during the experiments. The right insulated side represents the vertical symmetry plane of the pallet (no heat flux) and the left non-insulated side allows heat exchange with the ambient air (as for external sides of pallet). The top and the bottom are insulated in order to represent all product layers in a pallet except those at the top and the bottom, which have better heat exchange than the intermediate one. Air flows at a given air velocity through the crates by aspiration effect thanks to two fans. Thus, incoming airflow with low turbulence, such as that generally observed in a cold room, could be obtained. The airflow rate was adjusted by varying the

fan voltage between 6V and 24 V DC. Four current crates with a trapezoidal opening at the top (8.63 x 10^{-3} m^2) and the vent hole crates which are the current crates with two additional circular holes (2 x 1.26 x 10^{-3} m^2) on the left and the right were tested to study the effect of vent hole area. Because of the symmetry, the results for the other half of the pallet are considered to be the same.

Some tomatoes were instrumented at the core and on the surface by calibrated T-type thermocouples with an accuracy of ±0.2 °C (Fig. 2). The air temperatures were measured at the inlet (before crate 1) and at the outlet of the device (after crate 4), and inside the crates at about 3 cm from the surface of the instrumented tomatoes. A data logger (Agilent 34972A) and an acquisition software (DataLogger) monitored temperatures. Air velocity was measured using a hot wire anemometer (TESTO 435-4, velocity range 0-20 $m.s^{-1}$, accuracy $\pm 0.03\ \mathrm{m.s^{-1}}$). For current crate, the inlet air velocity was measured just only in front of the trapezoidal opening. For vent hole crate, the inlet air velocity was measured both in front of the trapezoidal opening and the vent holes. The average air velocity was calculated from five measurement positions, and each measurement was repeated 10 times with 1s interval between 2 records.

2.2. Experimental protocol

The test room temperature was set at a given temperature for about 6 h in order to obtain a homogeneous product temperature. Then, three additional polystyrene plates (0.04 m thickness) were placed at the left, the front and the rear of the device while the set temperature was changed. These plates were removed when the room temperature reached the new set value. Then, the fans were run and the experiment was immediately started by recording the air, surface and core temperatures every minute. In this manner, the product was protected from the external air during the lag time and the product temperature variation during the lag time can be considered as insignificant. The experiment was ended when the core temperature of the tomato located in crate 4 (encircled in black, Fig. 2) attained seven-eighths of the cooling temperature. This position was chosen because the heat exchange with air is expected to be the lowest. In the case where the

temperature dropped from 20 °C to 4 °C (cooling), the experiment was ended when the temperature of this tomato attained 6 °C. Conversely, when warming from 4 °C to 20 °C was conducted, the experiment was ended when its temperature reached 18 °C. The ambient temperatures of 20°C represent the average external temperature in a supply chain and 4°C represents the average temperature in cold equipment. It is to be emphasized that it took about 30 min. for the test room temperature to reach the new set value.

The influence of the following conditions on the product temperature was studied:

- Air velocity. The air velocity used in this study varied from 0 $\mathrm{m.s^{-1}}$(experiment of pallet filming) to 3.1 $\mathrm{m.s^{-1}}$ (maximum value often observed in a cold room). The air velocity of 0.15 and 0.30 $\mathrm{m.s^{-1}}$ represents the condition when a pallet is place in a calm ambient.

- Cooling (product at initial temperature of 20 °C exposed to air of 4 °C) and warming (product at initial temperature of 4 °C exposed to air of 20 °C).

- Crate vent area. Current crates and vent hole crates were tested.

- Filming. The device was completely covered by stretch cellophane film to represent a handling practice in the supply chain.

The experimental conditions are summarized in Table 1. The experiments 1 and 1' were carried out under the same conditions in order to verify the result repeatability. The product weight loss was considered as negligible during the experiment.

3. Model development

3.1. Heat transfer model

When a tomato (high initial temperature) was placed in a test room (low set temperature), the product temperature decreased and approached the set temperature. This is related to the heat transfer by conduction inside the tomato considered as a spherical object (radius R) and by

convection between the product surface and the external air. The heat transfer by radiation was considered as negligible in this study.

The heat flow, q (W), depends on the convective heat transfer coefficient, h (W.m^{-2}.K^{-1}), on the exchange area, S (m^2), and on the product thermal conductivity, λ (W.m^{-1}.K^{-1}).

The Biot number ($\mathrm{Bi} = \frac{hR}{\lambda} =$ ratio between internal and external heat transfer resistances) of tomato is about 0.4 (where R= 0.044 m, $\lambda = 0.61$ W.m^{-1}.K^{-1} and h ≈ 5 $\mathrm{W.m^{-2}.K^{-1}}$, see Table 2). This means that the internal heat transfer resistance due to the conduction inside the tomato cannot be neglected in comparison with the external one due to the convection.

An exact transient solution is available (Carslaw and Jaeger 1959), but a good approximation for a sphere can be obtained (van der Sman, 2003) by considering that the internal heat transfer resistance is approximately $\frac{R/4}{\lambda}$ whereas the external heat transfer resistance is $\frac{1}{h}$. Finally, the product core temperature change can be estimated using the following equation:

$$mC_p \frac{dT_c(t)}{dt} = \frac{1}{\frac{1}{h}+\frac{R}{4\lambda}} S(T_a - T_c(t)) \qquad (1)$$

where m = mass of one tomato [kg]

S= exchange area between product and air for one tomato [m^2]

C_p= thermal capacity of tomato [$\mathrm{J.kg^{-1}K^{-1}}$]

h = convective heat transfer coefficient [W.m^{-2}.K^{-1}]

$T_c(t)$ = product core temperature at time t [°C]

T_a= air temperature [°C]

If T_a is constant, which is almost the case for the inflowing air of crate 1, the product core temperature change over time can be represented in a dimensionless form as follows:

$$T_c^*(t) = \frac{T_c(t)-T_a}{T_0-T_a} = e^{-t/\tau} \qquad (2)$$

where $\tau = \frac{mC_p}{S}\left(\frac{R/4}{\lambda} + \frac{1}{h}\right) = \frac{mC_p}{hS}\left(1 + \frac{Bi}{4}\right)$ (3)

T_0 = initial product temperature [°C]

By tracing $\ln(T_c^*)$ as a function of time using the experimental data obtained from crate 1, a linear evolution is observed. The slope represents the inverse of the characteristic time τ. Then, the heat transfer coefficient h can be calculated.

In our study, a layer of a pallet is composed of 4 crates. In the case of product cooling, the air temperature increases when the air flows from the inlet of crate 1 (T_{a1}) to the outlet through the tomatoes located inside. The outlet temperature of crate 1 corresponds to the inlet temperature for crate 2 (T_{a2}). The airflow rate $\dot{m}_a$ is an influencing factor for the air temperature increase as shown below:

$$\dot{m}_a C_{p.air}(T_{a2}(t) - T_{a1}) = nS\frac{T_c(t) - T_{a1}}{\frac{R/4}{k} + \frac{1}{h}} \quad (4)$$

$T_{a1} =$ inlet air temperature of crate 1, considered as constant in our study

$T_{a2}(t) =$ outlet air temperature of crate 1 at time t, considered as the inlet temperature of crate 2.

$n =$ number of tomatoes in a crate = 12 in our study

So, eq. 4 can be used to calculate T_{a2}, T_{a3}, T_{a4} successively, given that T_{a1} is known.

Overall, the change in the product core temperature and the air temperature in different crates can be calculated by eq. 1 and 4.

3.2. Aroma model

A model predicting the evolution of the volatile compounds responsible for tomato aroma was developed as a function of the difference between the product temperature and the critical temperature (T_{cri}) of 12 °C as reported in Farneti et al. (2015). The model reasoning is also based on the results of several studies cited previously, i.e. the aroma volatile decreases at low temperature, and it is recovered only partially when the product is restored to an ambient temperature. There are

several pathways of volatile loss reaction in reality. However, our proposed model does not claim to reproduce the reaction scheme, it is only to reproduce Farneti's experimental results.

As a first approach, a set of first order kinetic reactions between three hypothetical chemical species is considered:

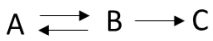

A: compound responsible for aroma

B: compound (without aroma) generated by reversible transformation of compound A

C: compound (without aroma) generated by irreversible transformation of compound B.

When the product temperature decreases below the critical value, A is transformed into B (A →B) and B is transformed into C (B→C). When the cold product is restored above the critical value, only B is transformed into A (B→A).

By considering the ratio of the aroma content at a given time and the initial content, the dimensionless values of A, B and C can be considered.

At the beginning (t = 0), A = 1, B = 0, C = 0.

At a given time t, the transformation reaction of A into B (and inversely) can be represented by the balance reaction equation of compound A:

$$\frac{dA(t)}{dt} = -k_1 \max\left(0, T_{cri} - T_c(t)\right) A(t) + k_2 \max(0, T_c(t) - T_{cri})\, B(t) \quad (5)$$

In eq. 5, when $T_c(t)$ is lower than T_{cri}, the first term applies: transformation of A into B. Conversely, when $T_c(t)$ is higher than T_{cri}, the second term applies: part of B is transformed back into A. This is related to the partial recovery of aroma.

The balance reaction equation of compound B is as follows:

$$\frac{dB(t)}{dt} = k_1 \max\left(0, T_{cri} - T_c(t)\right) A(t) - k_2 \max(0, T_c(t) - T_{cri})\, B(t) - k_3 \max\left(0, T_{cri} - T_c(t)\right) B(t) \quad (6)$$

The last term corresponds to the irreversible loss of aroma.

where k_1, k_2 and k_3 are kinetic parameters [$s^{-1}K^{-1}$]

The equations 5 and 6 represent hypothetic reactions, they have been chosen to reproduce literature data with a minimum number of reactions and parameters. In reality, more than three compounds could be involved in the reactions, higher order kinetics could apply and the variation kinetic parameters (k_1, k_2, k_3) could be non-linear.

4. Experimental results

4.1 Repeatability

Two experiments under the same conditions (Exp. 1 and Exp. 1', see Table 1) were carried out on different days. The changes in the inlet and outlet air temperatures, the average core temperature (calculated from five measurements) of crate 1 and crate 4 are shown in Fig. 3.

For both experiments, the air and product core temperatures decreased over time. Due to the regulation system, the inlet air temperature was initially slightly lower than the set temperature (3 °C instead of 4 °C). Then, it increased over time and reaches a stable value of 4 °C after about 120 min. Due to the product inertia, the core temperature decreased slowly at the beginning (until 15 min) then an asymptotic decrease was observed at around 4 °C. The outlet air temperature decreases form 12 °C to 4°C after about 180 min. Before 180 min, this outlet temperature was higher than that of the inlet temperature because air exchanges heat with the warm tomatoes when it flows through the crates.

A statistical analysis using Root Mean Square Error $\left(\mathrm{RMSE} = \sqrt{\frac{\sum_{i=1}^{n}(T_1 - T_1')^2}{n}}\right)$ was carried out where T_1 and T_1' are the core temperature measured at different times in the experiment 1 and 1', respectively and n is the number of measurements (300 for each experiment). RMSE was 0.5°C (for crate 1) and 0.2°C (for crate 4). These RMSE values are the same order of magnitude of the

thermocouple precision (±0.2°C), we can consider an acceptable repeatability for these two experiments. For facilitation, only one experiment was undertaken under the other conditions.

4.2 Product temperature heterogeneity

Fig. 4 shows the results obtained in Exp 1 at different positions at around half-cooling $\left(\text{when } \frac{T_c(t)-T_a}{T_0-T_a} \sim 0.5\right)$, where $T_c(t) =$ core temperature of the warmest tomato in crate 4 (circled in black) = 12.6 °C. Overall, the neighboring air temperature was lower than the surface temperature, which in turn was lower than the core temperature due to the convective heat transfer between air and the product surface and heat transfer by conduction inside the tomato. The differences in these temperatures are related to the Biot number of the tomato (= 0.4) as explained previously. The product temperature is not homogeneous, there is a difference between the core and surface temperatures.

Along the symmetry plane of the pallet, the air temperature increased from 6.7°C (crate 1) to 9.0°C (crate 4) because of convective heat exchange with the warm product (initial temperature 20°C) while flowing through the crates. On the external side of pallet where the crates are exposed to the ambient air, the air temperature fluctuated slightly, while that of crate 2 (7.4°C) and crate 4 (7.0°C) was lower than that of crate 1 (8.6°C) and crate 3 (8.9°C). This can be explained by the fact that the crate walls are not completely hermetic, there is external air infiltration (4°C) into crates 2 and 4, and this air mixes with the air coming from crates 1 and 3..

4.3. Difference between warming and cooling

In order to compare warming and cooling regimes, Exp 2 and Exp 3 were undertaken. For crate 1, Fig. 5 shows the dimensionless core temperature evolution defined as $T_c^*(t) = \frac{T_c(t)-T_a}{T_0-T_a}$. Considering forced convection, one should expect the same dimensionless temperature change during both warming and cooling regimes. However, these experiments were undertaken at a very low air velocity (0.15 $m.s^{-1}$), the large amount of heat exchange by natural convection explains the difference between warming and cooling curves. During warming, the warm lighter incoming air flowed above

the tomatoes almost without mixing with the cold air surrounding the tomatoes (Fig. 6), thus, low exchange. During cooling, incoming heavier cold air flowed downward and exchanged heat with the product, thus, better exchange.

4.4. Influence of air velocity

The results of various air velocities were analyzed: 0.15 $m.s^{-1}$, 1.0 $m.s^{-1}$, 2.0 $m.s^{-1}$, 2.2 $m.s^{-1}$ and 3.1 $\mathrm{m.s^{-1}}$ to highlight their influence. To overcome the slight difference in initial product temperature and air temperature in these experiments, the dimensionless core temperature change over time of the product located in crate 1 is presented in Fig. 7. The higher the air velocity, the higher the cooling rate of tomatoes. However, beyond 2.2 $m.s^{-1}$, this influence is not so obvious.

The convective heat transfer (h) was determined from these experiments. The logarithm of the dimensionless core temperature as a function of time of Exp 1 and Exp 1' are shown in Fig. 8 as example. The product inertia explains the lag time at the beginning. The determination of the slope (=1/ τ, see eq. 2) was carried out on the linear portion of the curve (2000s-18000s), which was then used to calculate h (see eq. 3).The determination of h for all experiments are presented in Table 1. It should be noted that h value identified from Exp 2 (warming regime) is slightly lower than that obtained in Exp 3 (cooling regime). This is due to the different airflow pattern (Fig. 6) and confirms the influence of natural convection.

Fig. 9 shows h versus Va for different air velocities. A power law, often proposed in the literature, was used to fit this curve as follows:

$$h=5.34.Va^{0.39} \quad (7)$$

This correlation, which applies for vent hole crate gives h = 1.38 $Wm^{-2}K^{-1}$ for Va = 0.3 ms^{-1} while that of current crate (Exp 7) gives h = 0.51 $Wm^{-2}K^{-1}$ for the same air velocity. This difference can be explained by the lower airflow rate throughout the tomatoes in current crate when the opening was located only at the top. This highlights the importance of the crate opening area.

4.5. Influence of filming

The experimental device was covered by stretch cellophane film (thickness of about 15 µ). The film limits the internal airflow, and thus, the air velocity can be considered as null (Va∼0 $m.s^{-1}$). Fig. 10 shows the dimensionless core temperature of crate 1 in the case of filming (Exp 8) compared with that of Va = 0.15 $m.s^{-1}$ (Exp 3). There is an obvious influence of the filming on the temperature decreases: the temperature is constant between 0 and 200 min because of the product inertia, then it decreases very slowly in comparison with the experiment where Va = 0.15 $m.s^{-1}$. Due to the poor heat exchange between air and the product in the filming case, the product temperature still does not reach stabilization state even at 2700 min. (about 2 days). It should be noted that in practice, the pallet is cooled without film and the filming takes place just before the transport stage.

It was observed that the vent hole crates (with two additional circular holes of 2 x 1.26 x 10^{-3} m^2) did not allow a significant increase in product cooling rate (result not shown).

5. Thermal model Validation

Eq. 1 and 4 were used to calculate the evolution of the mean core temperature in each crate and the outlet air temperature. The product initial temperature, the inlet air temperature and the air velocity were the model input parameter. Fig. 11 compares the model prediction and the measurement in terms of mean product temperature in create 1 and crate 4, air temperature at outlet of the pallet for an upstream air velocity of 2.2 $m.s^{-1}$ (mean upstream air temperature 4°C, initial product temperature 20°C). The trends are correctly predicted with acceptable reproducibility (RMSE for the product temperature is only 0.5°C). At the beginning of cooling, a short time delay before product temperature begins to decrease is observed experimentally. This delay is almost negligible compared to cooling time, thus, this is not taken into account in the proposed simplified model.

6. Identification of the kinetic coefficients of aroma transformation

Knowledge of the kinetic parameters k_1, k_2 and k_3 in the transformation reactions of the aroma compounds A, B and C, respectively is necessary for the prediction of the aroma evolution during the

supply chain. As a first approach, these coefficients were identified by fitting with the experimental results presented by Farneti et al. (2015) for the Amoroso (cocktail truss) and Cappricia (round truss) varieties. In this study, the tomatoes were stored firstly at 4.0 ± 0.5 °C (RH of 93 ± 7 %) in the dark, in open commercial cartons. At different times, 5, 10 and 15 days, a tomato batch previously stored at 4°C was placed in an environment at a temperature of 16 °C. Volatile analysis of the samples was assessed (by SPME/GC-MS technique) after zero, one, three and seven days at 16 °C. Hexanal was found to be the main volatile compound. Fig. 12 presents the experimental results of Amoroso concerning changes in the Hexanal fraction in test 1, 2, 3 and 4 (Cappricia not shown here). This figure also shows the best fitting curves (model 1, model 2, model 3 and model 4) considering the critical temperature (T_{cri}) of 12 °C. The identification of k_1, k_2 and k_3 from the fitting curves of Amoroso and Cappricia are reported in Table 3.

A statistical analysis using Root Mean Square Error (RMSE) was carried out by comparing the compound A (Hexanal) measured at different times by Farneti et al (2015) and the one predicted by our model. The discrepancy between the experimental and modelled results was 4.6% for Amoroso and 7.1% for Cappricia, thus, we considered as acceptable. The aroma data of Farneti et al. (2015) are related to a specific measurement procedure for two particular tomato varieties. The proposed aroma model, which uses only three adjusted parameters, was able to reproduce the aroma evolution under four different ambient temperatures. Thus, after validation by comparing with the published experimental data (Farneti et al., 2015), this model would be applied to other cold chain conditions. In continuation of this work, different product quality will be measured under different logistic chains by CTIFL (Centre Technique Interprofessionnel des Fruits et Légumes). These results will be helpful to develop more precise quality models.

In order to provide more information on the meaning of the kinetic parameters, the characteristic period during which the aroma decrease at 6 °C remains reversible can be obtained by calculating $1/(k_1.\Delta T)$ (for ΔT = 12°C-6 °C = 6 °C) which is about 20 days for Amoroso and 4 days for Cappricia. It seems that only a long storage period at a low temperature leads to significant aroma loss for the

Amoroso variety. The characteristic recovery time of aroma at 18 °C ($1/(k_2.\Delta T)$) is around 8 hours for both varieties.

The thermophysical properties of tomatoes used in the heat transfer modeling are presented in Table 2.

7. Numerical results of product temperature and aroma change in a supply chain

The heat transfer and aroma model were linked together to predict the product temperature and the aroma changes under different logistic conditions. Only the aroma evolution is shown (temperature evolution not shown) for two examples of supply chain scenarios : 'normal' and 'cold' scenario (Table 4).

Fig. 13 shows the evolution of aroma (compound A) and the irreversible aroma loss (compound C) for Amoroso and Cappricia varieties along the normal logistics chain. The aroma of Cappricia is influenced by the ambient temperature to a greater extent than that of Amoroso. Its aroma level (compound A) attains a minimum value of about 0.8 (20 % loss) at the end of stage 5 (supermarket cold room). This figure clearly shows that the aroma content decreases when the product is stored at a low temperature, particularly in a cold room or in a domestic refrigerator. The aroma is recovered when the product is placed at room temperature such as on a supermarket shelf and prior to consumption. The aroma evolution in stage 8 leads to a suggestion: the product should be returned to room temperature for about 1 day before being consumed. After 1 day, the aroma is almost completely recovered for the both varieties.

Fig. 14 shows the aroma evolution along the 'cold' logistics chain. The influence of low temperature on the aroma level and on the irreversible aroma loss is more noticeable in comparison with those in the 'normal' logistics chain. For the same logistics scenario, this influence is more significant for Cappricia than for Amoroso, particularly at the end of stage 5 (supermarket cold room) and stage 7 (domestic refrigerator). In spite of a 1-day period during which the tomatoes returned to room

temperature prior to consumption, the aroma recovery was only 75 % for Cappricia and 93 % for Amoroso.

8. Conclusion and perspectives

The importance of the air velocity on the convective exchange between air and product was observed, thus, on product temperature evolution. However, when the air velocity is higher than 2.2 $m.s^{-1}$, the role of air velocity on the product temperature change becomes insignificant. When the air velocity is very low (0.15 $m.s^{-1}$), the heat exchange by natural convection explains the lower rate of product temperature change when warming than when cooling. It was observed that the vent hole crates (with two additional circular holes of 2 x 1.26 x 10^{-3} m^2) did not allow a significant increase in product cooling rate. Entire pallet filming slows down drastically temperature change during cooling.

Relatively simple thermal and aroma models were developed and linked together. The simulation results highlight the influence of the ambient temperature and the duration of different stages in the logistics chain on the product temperature and the aroma content. The duration of the return to room temperature prior to consumption is a key factor because it influences the percentage of aroma recovery. It is to be emphasized that only thermal model was validated but not the aroma model because of a lack of experimental data to compare with the predicted results. Thus, only the trends and order of magnitude of aroma evolution in the logistic chain can be considered. Also, the kinetic parameters have to be further identified for other tomato varieties. The experimental study of quality evolution in progress consists in placing four varieties of tomatoes (Clodano, Deltary, Cauralina and Buffalo) in a test room in which the supply chain scenarios (based on field study) are simulated. Products are sampled at different times for quality analysis: physio-chemical (color, firmness, sugar content), organoleptic (aroma content, sensory test by trained consumer panel) and nutritional (Vitamin C, Carotenoids). Because of the heaviness of the quality measurement (HPLC and GC-MS for volatile component analysis, sensory analysis by consumer panel), the data of quality evolution under different cold chain scenarios will be available only in 2022. Then, the comparison

between the experimental results (including aroma evolution) and the prediction by model will be possible. After a validation of the aroma model and the calibration for specific tomato varieties, it could be applied in conjunction with the thermal model to analyze different supply chain scenarios. This analysis will be presented in the future work and some practical suggestions can be made for fruit and vegetable stakeholders and consumers.

Declaration of Competing Interest

The authors declare that they have no known competing financial interests or personal relationships that could have appeared to influence the work reported in this paper.

Acknowledgement

This study was carried out within the framework of the FreshQualiTom project benefiting a grant from the French Ministry of Agriculture (APP 2019 No. 19ART334141).

References

Ambaw A., Delele M.A., Defraeye T., Ho Q.T., Opara L.U., Nicolaï B.M., Verboven P., 2013, The use of CFD to characterize and design post-harvest storage facilities: Past, present and future, Computers and Electronics in Agriculture, 93, 184-194, http://dx.doi.org/10.1016/j.compag.2012.05.009.

Aubert, C., Baumann, S., Arguel, H., 2005. Optimization of the analysis of flavor volatile compounds by liquid− liquid microextraction (LLME). Application to the aroma analysis of melons, peaches, grapes, strawberries, and tomatoes. Journal of Agricultural and Food Chemistry, 53(23), 8881-8895, 10.1021/jf0510541

Bai, J., Baldwin, E. A., Imahori, Y., Kostenyuk, I., Burns, J., Brecht, J.K., 2011. Chilling and heating may regulate C6 volatile aroma production by different mechanisms in tomato (*Solanum lycopersicum*) fruit. Postharvest Biology and Technology, 60(2), 111–120, https://doi.org/10.1016/j.postharvbio.2010.12.002

Berry, T.M., Fadiji, T.S., Defraeye, T., Opara, U.L., 2017. The role of horticultural carton vent hole design on cooling efficiency and compression strength: A multi-parameter approach. Postharvest Biology and Technology, 124, 62-74, https://doi.org/10.1016/j.postharvbio.2016.10.005

Buttery, R.G., Teranishi R., Ling L.C., Flath R.A., Stern D., 1988. Quantitative studies on origins of fresh tomato aroma volatiles. Journal of Agricultural and Food Chemistry, 36, 1247-1250, 10.1021/jf00084a030

Carslaw, H.S., Jaege,r J.C., 1959. Conduction of Heat in Solids, 2nd edition, Oxford University Press.

Chourasia, M.K., Goswami, T.K., 2007. Steady state CFD modeling of airflow, heat transfer and moisture loss in a commercial potato cold store. International Journal of Refrigeration, 30, 672-689, https://doi.org/10.1016/j.ijrefrig.2006.10.002

Delele, M. A., Ngcobo, M. E. K., Getahun, S. T., Chen, L., Mellmann, J., Opara, U. L., 2013. Studying airflow and heat transfer characteristics of a horticultural produce packaging system using a 3-D CFD model. Part II: Effect of package design. Postharvest Biology and Technology, 86, 546–555, https://doi.org/10.1016/j.postharvbio.2013.08.015

de Leon-Sanchez, F.D., Pelayo-Zaldivar, C., Rivera-Cabrera, F., Ponce-Valadez, M., Avila-Alejandre, X., Fernandez, F.J., Escalona-Buendia, H.B., Perez-Flores, L.J., 2009. Effect of refrigerated storage on aroma and alcohol dehydrogenase activity in tomato fruit. Postharvest Biology and Technology, 54, 93–100, https://doi.org/10.1016/j.postharvbio.2009.07.003

Farneti, B., Alarcón, A.A., Papasotiriou, F.G., Samudrala, D., Cristescu, S.M., Costa, G., Harren, F.G.M, Woltering, E.J., 2015. Chilling-Induced Changes in Aroma Volatile Profiles in Tomato. Food Bioprocess Technology, 8, 1442–1454, DOI 10.1007/s11947-015-1504-1.

Gomez, P., Ferrer, M. A., Fernandez-Trujillo, J. P., Calderon, A., Artes, F., Egea-Cortines, M., Weiss, J., 2009. Structural changes, chemical composition and antioxidant activity of cherry tomato fruits (cv. Micro-Tom) stored under optimal and chilling conditions. Journal of the Science of Food and Agriculture, 89, 1543–1551, **https://doi.org/10.1002/jsfa.3622**

Li, J., Di, T., Bai J., 2019, Distribution of Volatile Compounds in Different Fruit Structures in Four Tomato Cultivars, Molecules, 24(14)2594, 10.3390/molecules24142594.

Moureh, J., Flick, D., 2004. Airflow pattern and temperature distribution in a typical refrigerated truck configuration loaded with pallets, International Journal of Refrigeration, 27, 464-474, doi:10.1016/j.ijrefrig.2004.03.003

Pham, A. T., Moureh, J., Flick, D., 2019. Experimental characterization of heat transfer within a pallet of product generating heat. Journal of Food Engineering, 247, 115-125, https://doi.org/10.1016/j.jfoodeng.2018.12.003

Pham, A. T., Moureh, J., Belaidi, M., Flick, D., 2021, CFD modelling of a pallet of heat-generating product applied to a cheese product, International Journal of Refrigeration, 128, 163-176, https://doi.org/10.1016/j.ijrefrig.2021.03.011

Raffo, A., Masci, M., Moneta, E., Nicoli, S., del Pulgar, J. S., & Paoletti, F., 2018. Characterization of volatiles and identification of odor-active compounds of rocket leaves. Food chemistry, 240, 1161-1170, https://doi.org/10.1016/j.foodchem.2017.08.009

Renard, C., Ginies, C., Gouble, B., Bureau, S., Cause, M., 2013. Home conservation strategies for tomato (*Solanum lycopersicum*): Storage temperature vs. duration – Is there a compromise for better aroma preservation? Food Chemistry, 139, 825-836, http://dx.doi.org/10.1016/j.foodchem.2013.01.038.

Saltveit, M.E., Morris, L.L., 1990. Overview on chilling injury of horticultural crops. In: Wang, C.Y. (Ed.), Chilling Injury of Horticultural Crops. CRC Press, Boca Raton.

Sweat, V.E., 1995. Thermal Properties of Foods, In: Eng. Prop. Foods, Marcel Dekker Inc. - ed. 2; 99-138.

Tandon, K.S., Baldwin E.A., Shewfelt R.L., 2000, Aroma perception of individual volatile compounds in fresh tomatoes (Lycopersicon esculentum, Mill.) as affected by the medium of evaluation, Postharvest Biology and Technology, 20(3), 261-268, https://doi.org/10.1016/S0925-5214(00)00143-5.

Tapsoba, M., Moureh, J., Flick, D., 2006. Airflow patterns in an enclosure loaded with slotted pallets, International Journal of Refrigeration, 29, 899-910, https://doi.org/10.1016/j.ijrefrig.2006.01.011

Wang, L., Baldwin, E., Luo, W., Zhao, W., Brecht, J., Baib, J., 2019, Key tomato volatile compounds during postharvest ripening in response to chilling and pre-chilling heat treatments, Postharvest Biology and Technology, 154, 11-20, https://doi.org/10.1016/j.postharvbio.2019.04.013

van der Sman, R.G.M., 2003. Simple model for estimating heat and mass transfer in regular-shape foods. Journal of Food Engineering, 60, 383-390, https://doi.org/10.1016/S0260-8774(03)00061-X

Zhang, Z. M., Zeng, D. D., Li, G. K., 2008. Study of the volatile composition of tomato during storage by a combination sampling method coupled with gas chromatography/mass spectrometry. Journal of the Science of Food and Agriculture, 88(1), 116–124, **https://doi.org/10.1002/jsfa.3054**

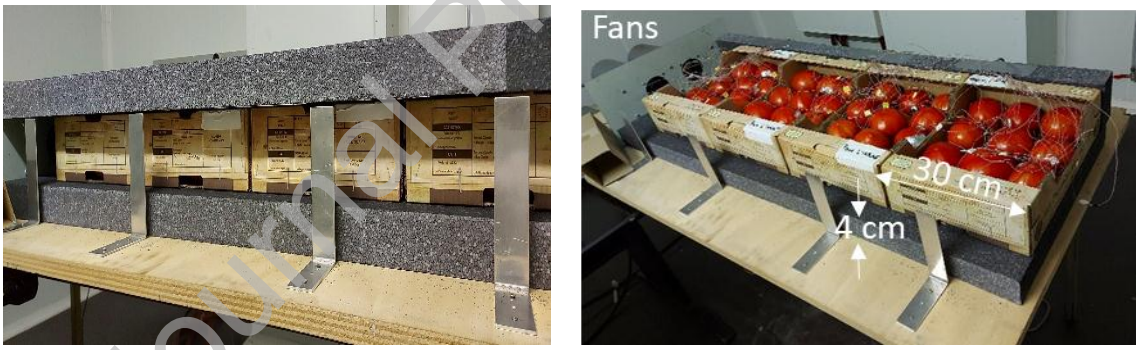

(a) (b)

Fig 1. Experimental device representing a half-layer of tomato crates in a pallet

(a) Experimental device during the experiment with a polystyrene plate at the top to simulate all the product layers in a pallet with the exception of the top/bottom ones

(b) Experimental device before the experiment (without a polystyrene plate at the top in order to show product arrangement and thermocouples)

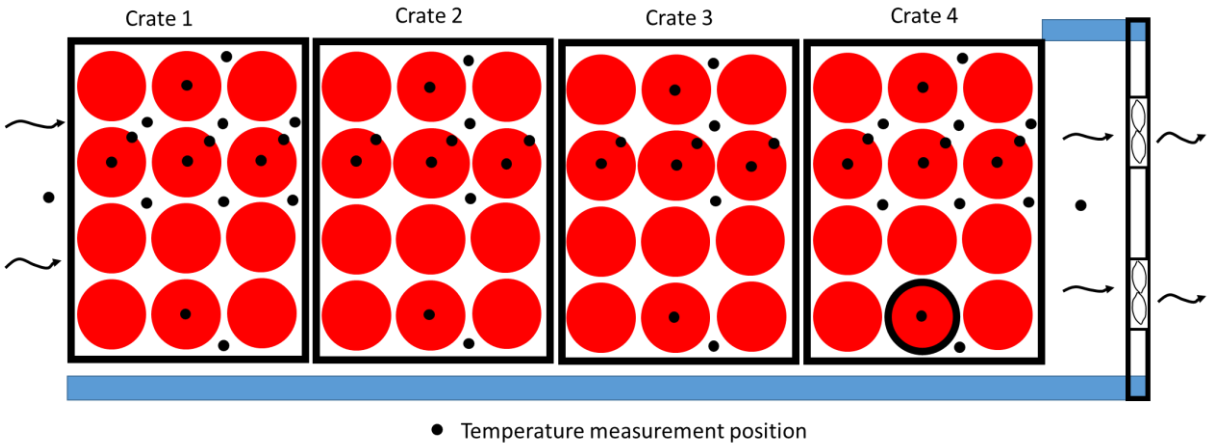

Fig 2. Top view of the experimental device showing the positions of air, core and surface temperature measurements

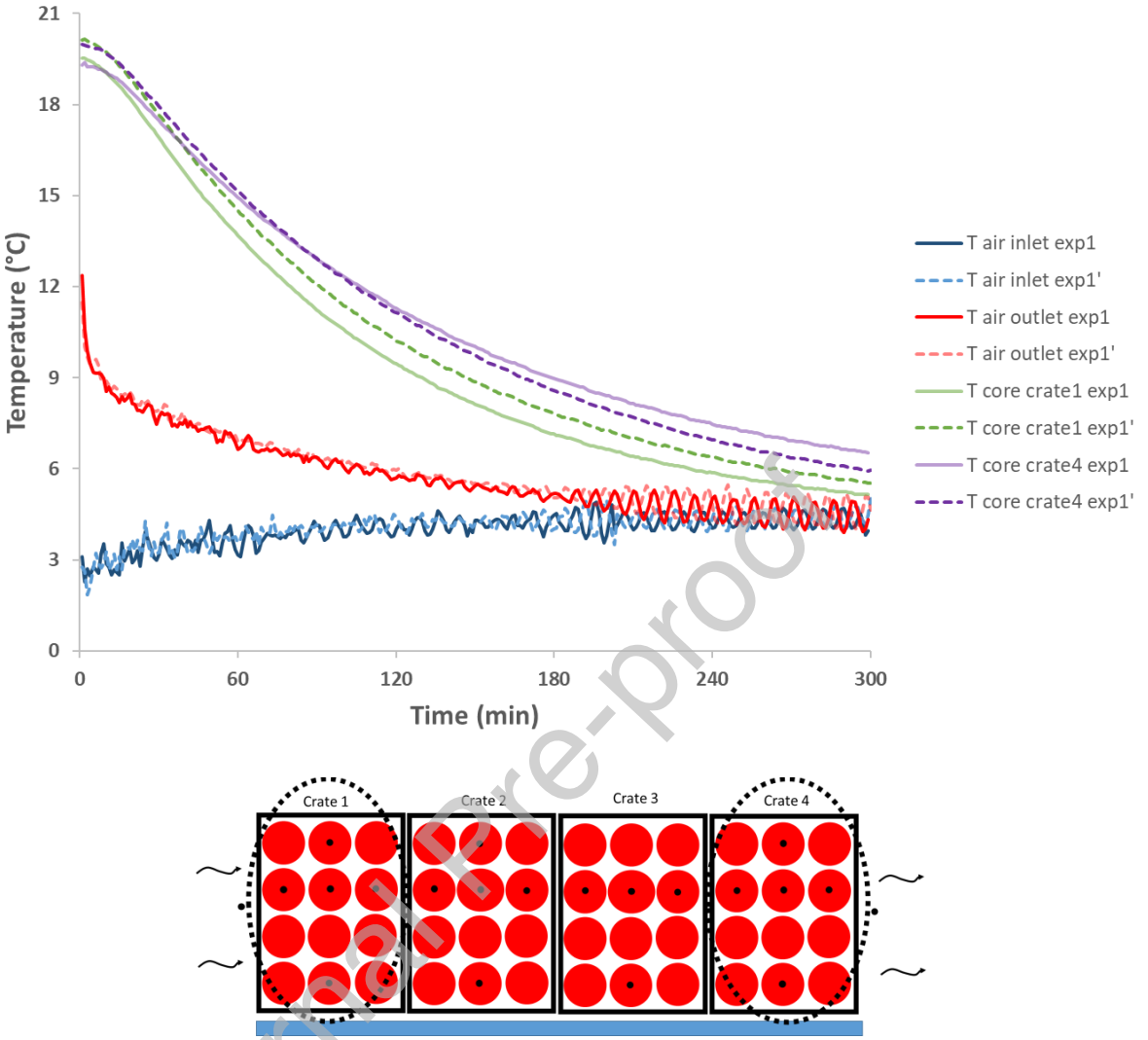

Fig 3. Average core temperature of crates 1 and 4 in two experiments performed under the same conditions (test room temperature 4 °C, initial product temperature 20 °C, Va = 2.2 $m.s^{-1}$, circular holes open)

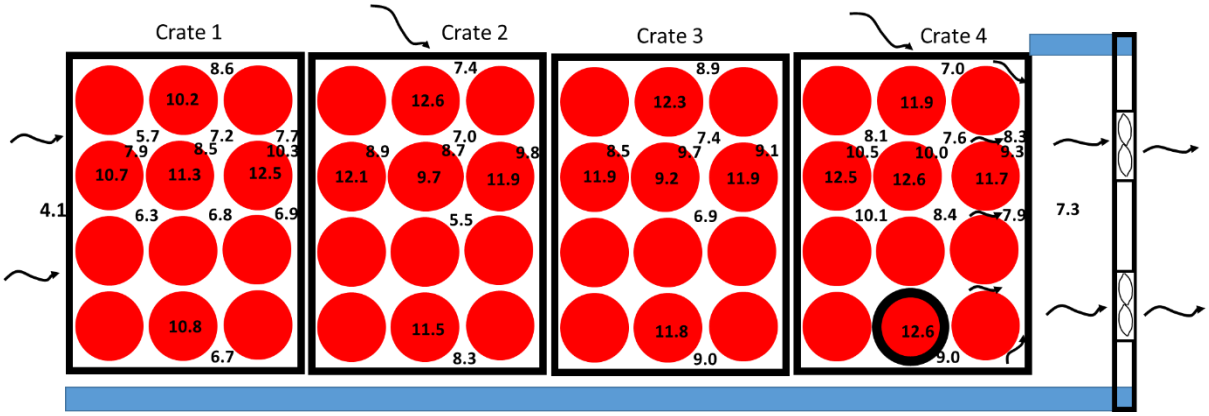

Fig 4. Top view of the experimental device showing the distribution of air, surface and core temperatures at half-chilling during Experiment 1 (test room temperature 4.0 °C, initial product temperature 19.5 °C, Va = 2.2 m/s, circular holes open)

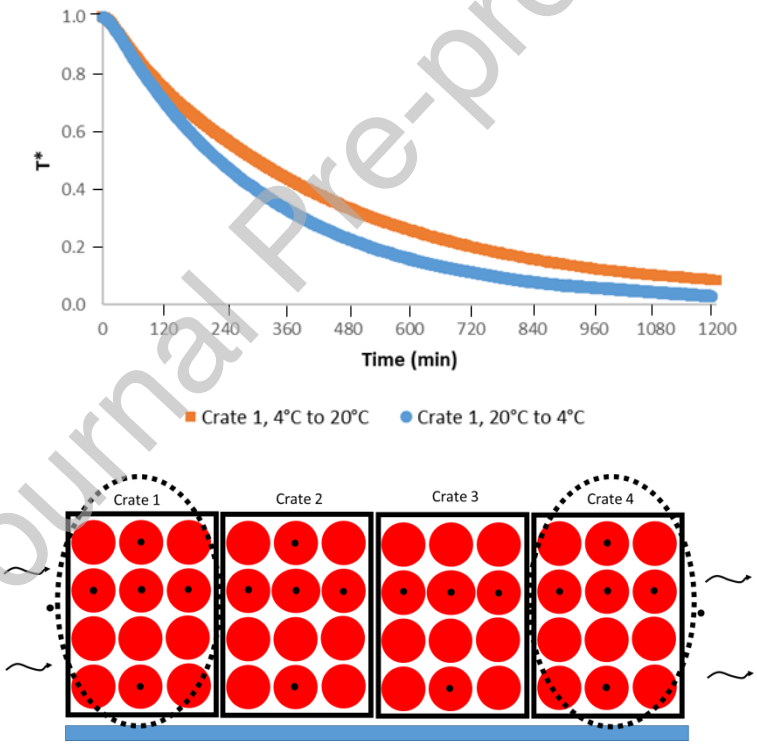

Fig 5. Dimensionless core temperature change (average value of 5 instrumented tomatoes in a crate) during warming with a low air velocity of 0.15 $m.s^{-1}$ (■ initial product temperature of 4.5 °C exposed to air at a temperature of 20.4 °C), and during cooling (● initial product temperature 19.9 °C exposed to air at a temperature of 4.6 °C) (a) crate 1 (b) crate 4.

Side view of airflow during warming ■ Side view of airflow during coolng ■

Fig 6. Schematic airflow during product warming and during product cooling

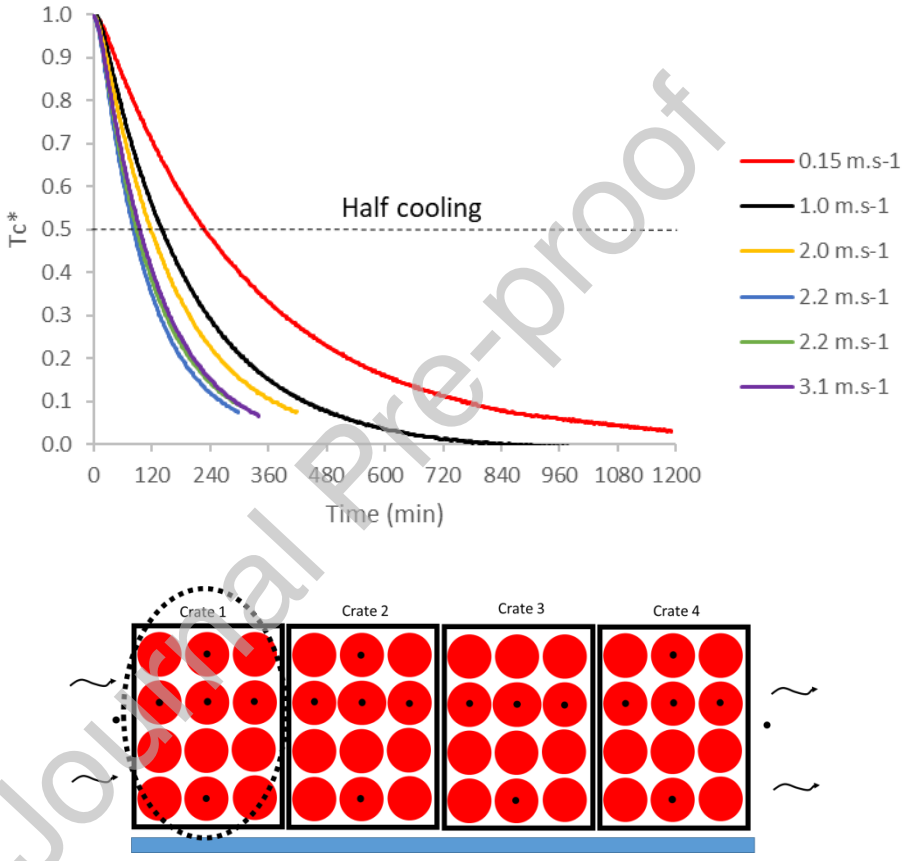

Fig 7. Influence of air velocity on the dimensionless core temperature of crate 1 (average of five measurements) for product initial temperature of about 20 °C and air temperature of about 4 °C.

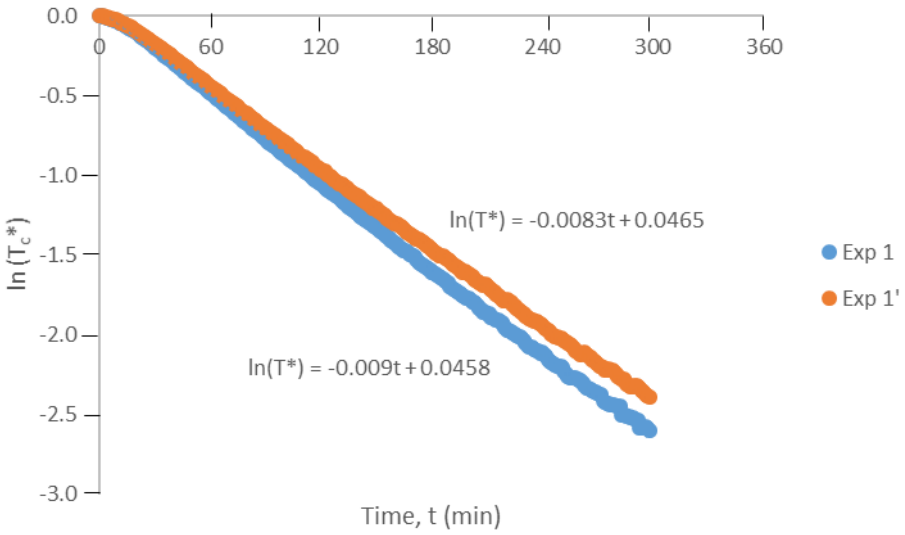

Fig 8. Logarithm of the dimensionless core temperature of product in crate 1 $\ln(T_c^*)$ as a function of time (t) for Experiments 1 and 1'.

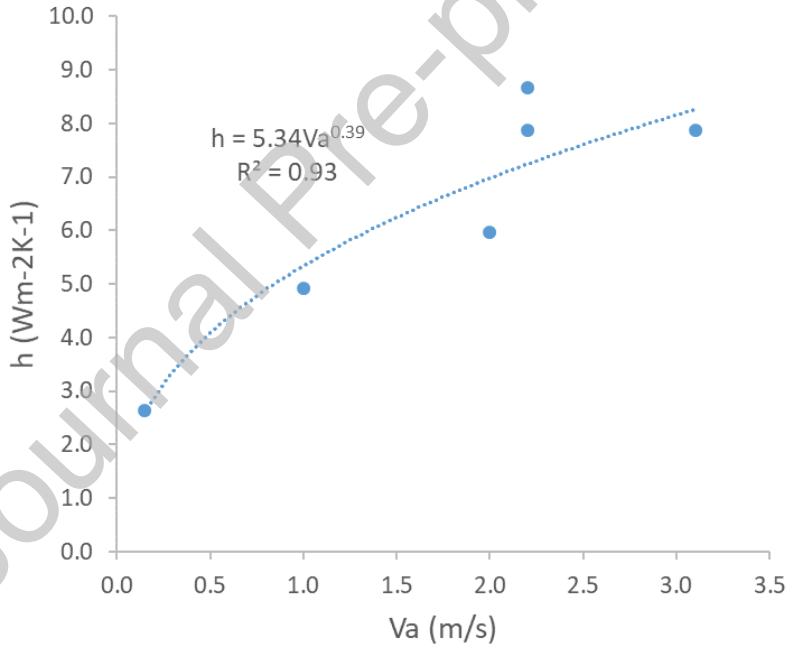

Fig 9. Correlation between the convective heat transfer coefficient and air velocity for product cooling from around 20 °C to around 4 °C, with the vent hole crate.

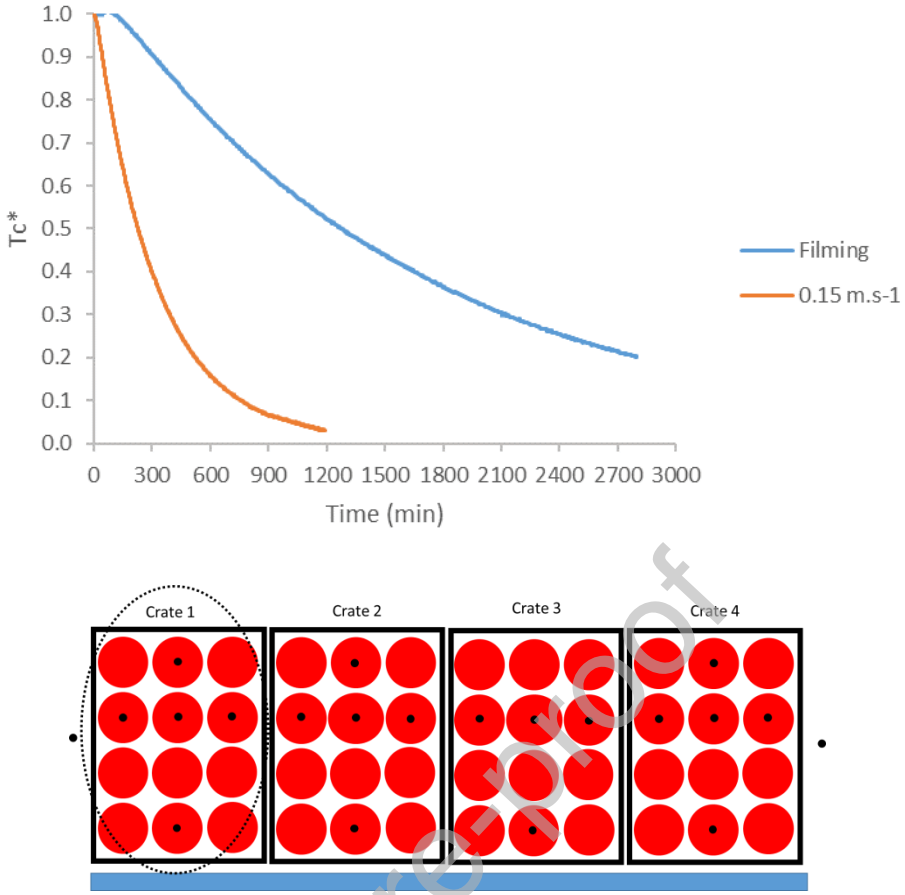

Fig 10. Influence of filming in comparison with the experimental results concerning an air velocity of $0.15\ \mathrm{m.s^{-1}}$.

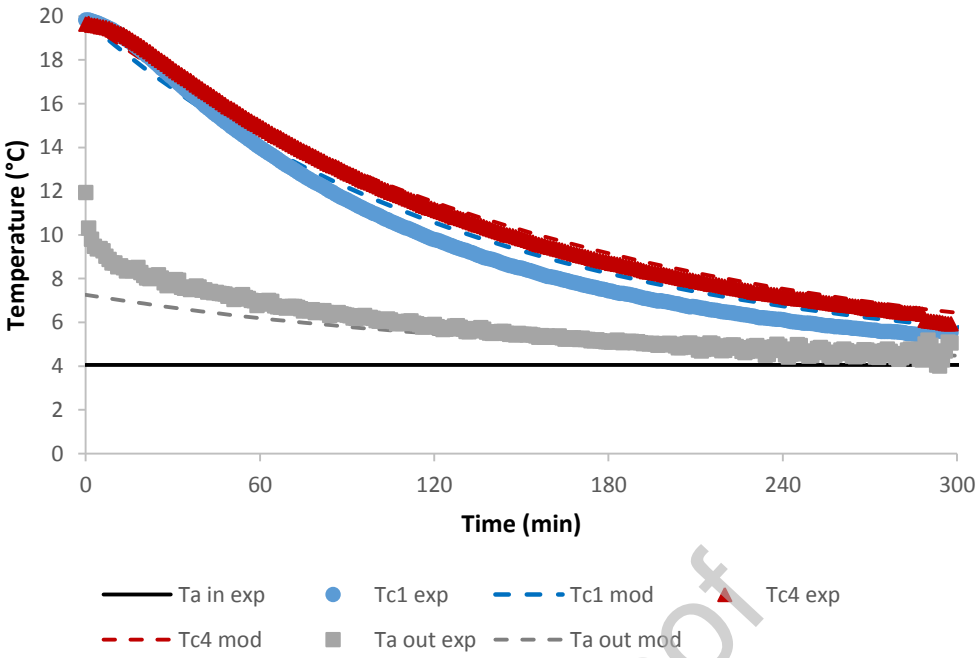

Fig 11. Comparison between the mean core temperature of the crates 1 and 4 and the outlet air temperature (downstream of crate 4) for the experiment 1 (product initial temperature 20°C, inlet air temperature 4°C and air velocity 2.2 $m.s^{-1}$).

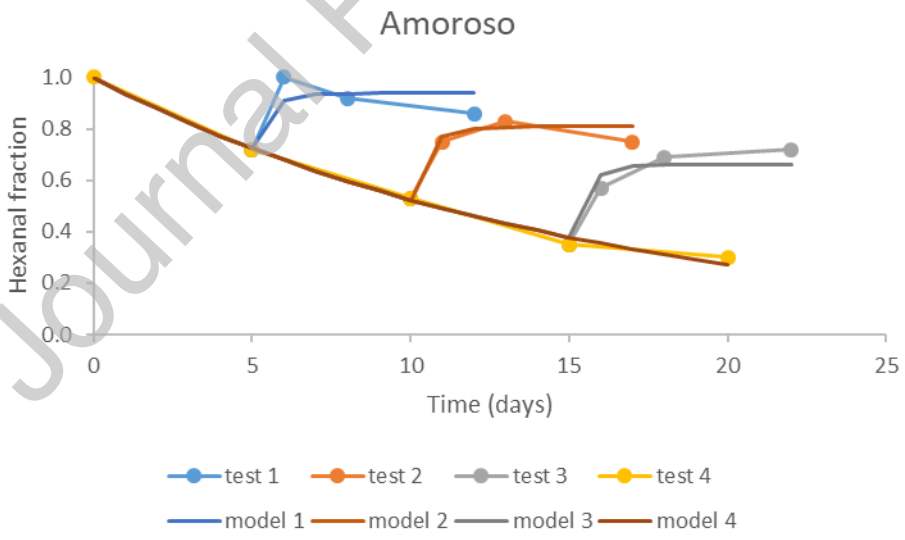

Fig 12. Experimental results of Amorosso variety (Farneti et al. 2015) for Hexanal evolution during storage in test 1 (5 days at 4 °C + 7 days at 16 °C), test 2 (10 days at 4 °C + 7 days at 16 °C), test 3 (15 days at 4 °C + 7 days at 16 °C) and test 4 (20 days at 4 °C) in comparison with the best fitting curves (model 1, model 2, model 3 and model 4).

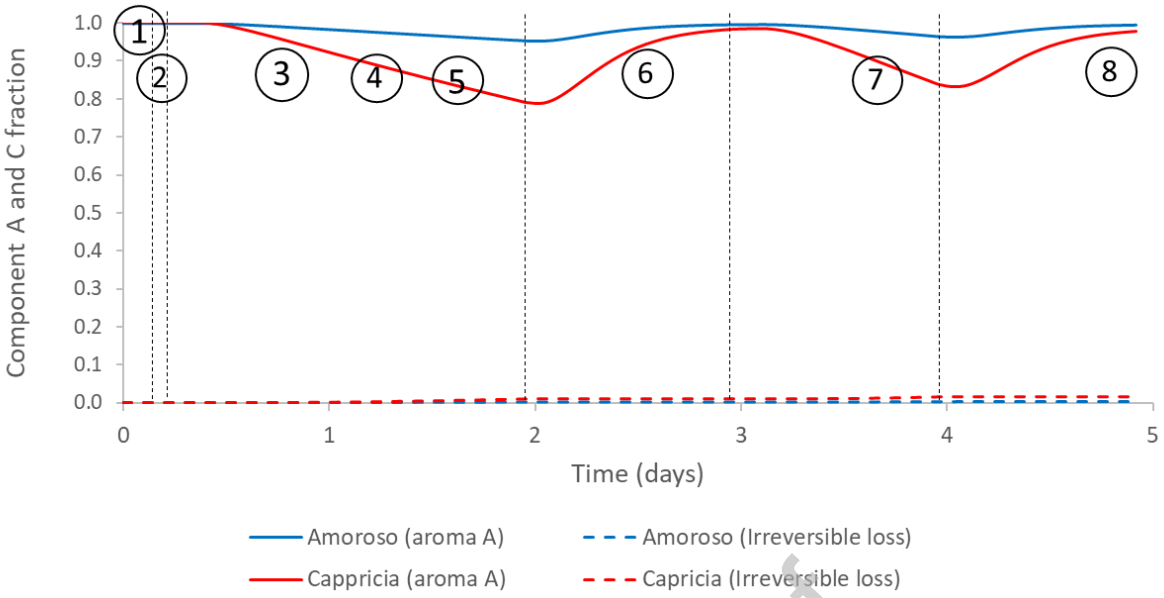

Fig 13. Numerical results for aroma changes in Amoroso and Cappricia varieties in the example of a normal logistics chain

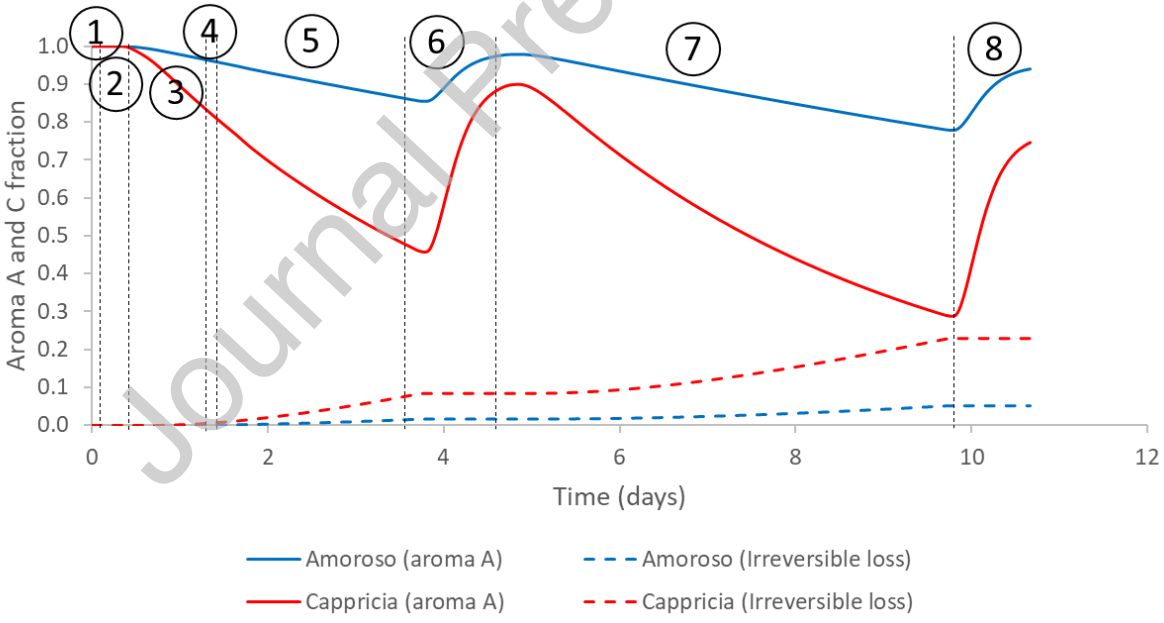

Fig 14. Numerical results for aroma change in the example of a cold logistics chain for Amoroso and Cappricia varieties

Table 1. Experimental conditions under which the experiments were carried out in this study

Exp. No.	Initial product temperature (°C)	Inlet air temperature (°C)	Inlet air velocity (m/s)	Crate type	Filming	h ($W.m^{-2}.K^{-1}$)
1	19.5	4.0	2.2	Vent hole	No	8.68
1’	20.1	4.1	2.2	Vent hole	No	7.87
2	4.5	20.4	0.15	Vent hole	No	2.08
3	19.9	4.6	0.15	Vent hole	No	2.63
4	20.1	4.5	1.0	Vent hole	No	4.92
5	19.3	4.1	2.0	Vent hole	No	5.96
6	18.9	4.3	3.1	Vent hole	No	7.87
7	21.2	4.5	0.3	Current	No	0.51
8	19.7	- (vary with time)	0	Current	Yes	-

Table 2. Thermophysical properties used in the heat transfer modeling.

Parameter	Value	Source
R |m]	0.044	Measurement
S [m^2]	0.0243	Calculation
m [kg]	0.307	Measurement
ρ $[kg.m^3]$	1028	Measurement
λ $[W.m^{-1}.K^{-1}]$	0.61	Sweat (1995)
C_p $[J.kg^{-1}.K^{-1}]$	3980	Sweat (1995)

Table 3. k_1, k_2 and k_3 values used in aroma modeling (values identified from the experimental results obtained by Farneti et al. (2015)).

Tomato variety	k_1 ($d^{-1}.K^{-1}$)	k_2 ($d^{-1}.K^{-1}$)	k_3 ($d^{-1}.K^{-1}$)
Amoroso	0.0081	0.493	0.0126
Cappricia	0.0403	0.493*	0.0159

*assumed to be the same as for Amoroso

Table 4. Two examples of scenarios in the tomato logistics chain used for the simulation **(stages with different conditions)**

Stage No.	Stage	Normal logistics chain (Example 1)			Cold logistics chain (Example 2)			Configura-tion
		Amb. Temp. (°C)	Va ($m.s^{-1}$)	Duration (h)	Amb. Temp. (°C)	Va ($m.s^{-1}$)	Duration (h)	
1	Producer's or shipping station	15	0.5	6	15	0.5	6	pallet
2	**Transport in a trailer**	8	**0.5**	8	8	**1**	8	pallet
3	**Wholesale/logistics platform**	**8**	0.5	24	**6**	0.5	24	pallet
4	**Transport in a trailer**	8	0.5	2	**4**	0.5	2	pallet
5	**Supermarket cold room**	**8**	0.5	**6**	**6**	0.5	**48**	pallet
6	Display on a shelf in a supermarket	20	0.2	24	20	0.2	24	individual crate
7	**Home storage in a domestic refrigerator**	6	0.2	**24**	6	0.2	**5*24**	individual tomatoes
8	Return to ambient	20	0.2	24	20	0.2	24	individual

	temperature prior to consumption							tomatoes